ACS APPLIED MATERIALS & INTERFACES

Research Article

www.acsami.org

Fabrication of Ultrasensitive Field-Effect Transistor DNA Biosensors by a Directional Transfer Technique Based on CVD-Grown Graphene

Chao Zheng,[†] Le Huang,[‡] Hong Zhang,[§] Zhongyue Sun,[†] Zhiyong Zhang,*[,‡] and Guo-Jun Zhang*[,†]

[†]School of Laboratory Medicine and [§]Teaching and Research Office of Forensic Medicine, Hubei University of Chinese Medicine, 1 Huangjia Lake West Road, Wuhan 430065, P.R. China

[‡]Key Laboratory for the Physics and Chemistry of Nanodevices, Department of Electronics, Peking University, Beijing 100871, P.R. China

Supporting Information

ABSTRACT: Most graphene field-effect transistor (G-FET) biosensors are fabricated through a routine process, in which graphene is transferred onto a Si/SiO_2 substrate and then devices are subsequently produced by micromanufacture processes. However, such a fabrication approach can introduce contamination onto the graphene surface during the lithographic process, resulting in interference for the subsequent biosensing. In this work, we have developed a novel directional transfer technique to fabricate G-FET biosensors based on chemical-vapor-deposition- (CVD-) grown single-layer graphene (SLG) and applied this biosensor for the sensitive detection of DNA. A FET device with six individual array sensors was first fabricated, and SLG obtained by the CVD-growth method was transferred onto the sensor surface in a directional manner. Afterward, peptide nucleic acid (PNA) was covalently immobilized on the graphene surface, and DNA detection was realized by applying specific target DNA to the PNA-functionalized G-FET biosensor. The developed G-FET biosensor was able to detect target DNA at concentrations as low as 10 fM, which is 1 order of magnitude lower than those reported in a previous work. In addition, the biosensor was capable of distinguishing the complementary DNA from one-base-mismatched DNA and noncomplementary DNA. The directional transfer technique for the fabrication of G-FET biosensors is simple, and the as-constructed G-FET DNA biosensor shows ultrasensitivity and high specificity, indicating its potential application in disease diagnostics as a point-of-care tool.

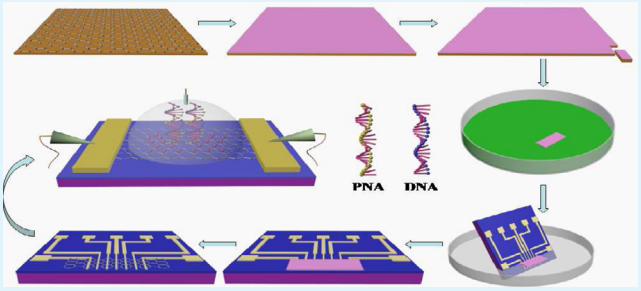

KEYWORDS: *graphene, field-effect transistor biosensor, directional transfer technique, peptide nucleic acid-DNA hybridization, detection*

INTRODUCTION

Graphene is a two-dimensional honeycomb lattice of carbon with an sp^2 structure that exhibits amazing physical and chemical properties for biosensing, such as high intrinsic carrier mobility, ultrathin body, ambipolar effect, low intrinsic noise level, good biocompatibility, and stability.[1−3] Rapid and highly sensitive detection of DNA is quite important for disease diagnosis, environmental monitoring, and so on.[4−6] Conventional DNA detections including real-time polymerase chain reaction (PCR) are tedious operations and require labeling with fluorescent dye. Recently, graphene-based optical and electrochemical transduction platforms have been developed,[7,8] in which fluorescence or electrochemical tags are still required. In contrast, graphene field-effect transistor (G-FET) biosensors hold particular advantages for detecting nucleic acids, because they do not require fluorescent labels or electrochemical tags and achieve high sensitivity, specificity, and rapid measurement.[2,9,10] Therefore, there is a significant need for the rapid and cost-effective production of high-quality G-FET devices.

A rapid and economical method for preparing high-quality graphene is a very important process for the fabrication of graphene devices. Currently, there are three major types of methods for preparing graphene that is subsequently used in FET biosensor fabrication. These methods include the production of graphene flakes obtained by micromechanical exfoliation from graphite,[1,11,12] the production of reduced graphene oxide (RGO) by the reduction of liquid exfoliation of graphite,[13−15] and the production of chemical-vapor-deposition- (CVD-) grown graphene.[16−18] In the case of micromechanical exfoliation, the pristine graphene obtained by micromechanical cleavage of graphite with tape demonstrates the best electronic and structural qualities. However, this approach is time-consuming and yields uncontrollable graphene devices in terms of shape, size, and location. The drop-casting[10] or spin-coating[19,20] technique provides the potential for assembling RGO-based FET biosensors. Nevertheless, the size and number of layers of the resulting RGO are not yet controllable, so it is difficult to obtain a single layer of RGO.

Received: January 13, 2015
Accepted: July 23, 2015
Published: July 23, 2015

DOI: 10.1021/acsami.5b03941
ACS Appl. Mater. Interfaces 2015, 7, 16953−16959

Because all oxygen groups on the GO surface cannot be completely removed during the reduction process, the mobility and conductivity of the resulting RGO are still lower than those of CVD-grown graphene. The CVD method prepares large-scale high-quality monolayer graphene and is an economical and promising appraoch. It is believed that high-yield and high-quality CVD graphene enables the mass production of electronic sensors with high sensitivity and high reproducibility.

Many efforts have recently been directed toward the fabrication of CVD-grown graphene FET biosensors for label-free DNA detection with high sensitivity. For example, Guo et al.[21] reported a label-free DNA FET biosensor based on CVD-grown graphene, achieving a detection limit of 1 nM. Dong et al.[22] reported a liquid-gated FET biosensor based on few-layer CVD-grown graphene for label-free DNA detection, in which the detection limit for complementary DNA could be as low as 10 pM. Chen et al.[23] developed a gold transfer technique to fabricate a CVD-grown monolayer graphene FET biosensor, in which DNA detection could be achieved down to 1 pM. In that work, although the fabrication process was rapid because of the use of silver paste as electrodes, the contact between graphene and silver paste, including the adhesion strength and contact resistant, is still uncontrollable. Recently, Xu et al.[24] employed an amplification strategy combined with CVD-grown graphene to realize 100 fM DNA detection. However, it is well-known that the CVD-grown graphene FET devices are usually fabricated by conventional techniques.[25,26] A flow diagram of the conventional G-FET fabrication process is shown in Scheme S1. As can be seen, the fabrication process of each single chip is complex. For one run, only one G-FET chip can be fabricated by the overall fabrication process. As a result, the manufacturing flow suffers from time-consuming and costly fabrication. On the other hand, cleanliness of the graphene surface is extremely important, because residual contamination on the graphene surface affects the functionalization of biological species and the intrinsic properties of graphene.[2,27] Very recently, Lerner et al.[28] proposed a transfer method of patterning a graphene nanoribbon for the scalable production of nanosensors to detect proteins with high sensitivity. However, this method still suffers from complex operation processes and requirements of professional technical personnel.

In this work, we have developed an ultrasensitive CVD-grown single-layer graphene (SLG) FET DNA biosensor by a novel directional transfer technique, in which CVD-grown monolayer graphene is transferred onto a prefabricated sensor array surface in a directional manner (Scheme 1). A 4-in. wafer containing 110 devices is fabricated at one time by the microfabrication process, after which the G-FET device is obtained by the directional transfer technique. To our knowledge, this is the first example of the use of a directional transfer technique to fabricate a peptide-nucleid-acid- (PNA-) functionalized graphene FET biosensor for DNA detection. Compared to conventional techniques, the directional transfer technique presents the following outstanding advantages: (1) high yield, as 160 G-FET devices were fabricated in this work and 144 of them worked normally (yield = 90%); (2) simple operation and reduced time, as one G-FET chip can be fabricated during the whole run in the conventional fabrication process whereas graphene can be transferred onto prefabricated wafer-scale chips for fabrication of G-FET chips by the directional transfer technique; (3) cost-effective process, as a 1×1 cm^2 SLG/copper sample could be used for the fabrication of about 100 devices; and (4) clean graphene surface, as poly(methyl methacrylate) (PMMA) is used only once, whereas PMMA must be used three times in the conventional approach.

Scheme 1. Schematic Illustration of the Directional Transfer Technique Process for the Fabrication of a Graphene-Based FET Biosensor[a]

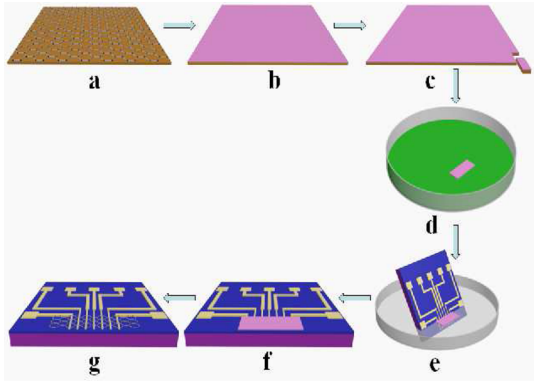

[a]Steps: (a) Single-layer graphene (SLG) grown on 1×1 cm^2 copper by CVD. (b) PMMA coated on SLG/copper by a spin-coater. (c) PMMA/SLG/copper cut into small pieces with scissors, as desired. (d) Small piece of PMMA/SLG/copper immersed into etchant to remove copper. (e) PMMA/SLG directionally transferred onto the FET chip, where the sensing array is located. (f) PMMA/SLG transferred to the sensing array surface by the directional transfer technique. (g) G-FET obtained by treatment with hot acetone (60 °C) overnight and subsequent thermal annealing at 200 °C in a vacuum to decompose PMMA.

EXPERIMENTAL METHODS

Materials. The 22-mer PNA probe sequence was synthesized by Bio-Synthesis, Inc. (Lewisville, TX). The 22-mer DNAs were purchased from Takara Biotechnology Co. Ltd. (Dalian, China) and were purified by high-performance liquid chromatography (HPLC). All PNAs and DNAs were dissolved in 1 × phosphate-buffered saline (PBS) buffer solution. The sequence of the PNA probe was N-AACCACACAACCTACTACCTCA-C. The hybridization sequences of DNAs in use were as follows: 5′-TGAGGTAG-TAGGTTGTGTGGTT-3′ (complementary, cDNA), 5′-TGAGG-TAGTAGGATGTGTGGTT-3′ (one-base-mismatched), and 5′-ATG-CATGCATGCATGCATGCAA-3′ (noncomplementary, non-DNA). 1-Pyrenebutanoic acid succinimidyl ester (PASE) and ethanolamine (EA) were obtained from Sigma-Aldrich. Ultrapure water obtained from a Millipore water purification system (18.2 MΩ resistivity, Milli-Q Direct 8) was used throughout the research.

Growth of Graphene on the Copper Foil Surface by Chemical Vapor Deposition. Graphene films were grown by atmospheric-pressure CVD on 25-μm copper foils (Alfa Aesar, 99.8% purity) using a growth method that has been described elsewhere.[29] Briefly, copper foil was placed in a tube furnace and heated at 1070 °C under a flow of 300 sccm hydrogen for 50 min to remove the native oxide of copper. Then a mixture of 5 sccm methane and 700 sccm hydrogen was introduced into the quartz tube to grow graphene for 30 min. Subsequently, the quartz tube was removed from the heating region of the furnace so that the copper foil was rapidly cooled for monolayer graphene formation.

Fabrication of G-FETs by the Directional Transfer Technique. To make it convenient for transferring graphene onto the biosensor array, the biosensor array was fabricated on the edge of the chip surface. By the conventional microfabrication technology, the source and drain electrodes were well fabricated on a 285-nm SiO_2/Si substrate by photolithography, followed by electron beam evaporation deposition of 5 nm/45 nm Ti/Au. To strengthen the adhesion between the Au and the Si wafer, a 5-nm-thick Ti layer was used.

DOI: 10.1021/acsami.5b03941
ACS Appl. Mater. Interfaces 2015, 7, 16953−16959

To transfer graphene from copper substrates to the FET chip substrates, a PMMA solution was spin-coated onto the SLG/copper foils at 4000 rpm for 30 s and dried in air. The 1 × 1 cm^2 PMMA/SLG/copper sample was cut into about 100 small pieces with scissors (approximately 1 × 1 mm^2 for one cut graphene sheet). The copper substrate was etched away using Cu etchant [mixture of copper sulfate, hydrochloric acid, and deionized (DI) water] for about 15 min. It is interesting that the directional transfer technique process required a shorter Cu etching time (ca. 15 min) than the conventional transfer technique (ca. 2 h). This is mainly because of the small size of the cut PMMA/SLG/copper samples. Isopropyl alcohol (IPA)/DI water (1:10) was used to wash the chip three times to remove the etchant residue.[30,31] PMMA/SLG was directionally transferred onto the top of the biosensor array surface of the prefabricated electrode devices by aligning the small PMMA/SLG sample with the array surface in solution. Compared to the conventional method, the alignment could be realized in solution, simplifying the fabrication process. Prior to the transfer process, the FET channel surface was functionalized with 3-aminopropyltriethoxysilane (APTES),[29,32] which is extremely important for making the transferred graphene completely stable on the SiO_2 surface through strong interactions between the amino groups and graphene. Then, the PMMA/SLG/SiO_2 stack was annealed at 220 °C for about 5 min on a hot plate,[33] to minimize the wrinkles that inevitably formed during the transfer process and enhance the contact between the SLG and SiO_2/Si substrate. Finally, to make the graphene surface as clean as possible, the PMMA layer was removed using hot acetone (60 °C) overnight, and then the SLG/SiO_2/Si substrate was annealed in a vacuum at 200 °C for 2 h to decompose the polymers.[23,34] Because the PMMA polymer was used only once, the residual polymer on the graphene surface was easily removed.

Functionalization of G-FET Biosensor. PASE was used as a cross-linker to immobilize PNA on the graphene surface. First, the chip was immersed in PASE in dimethyl sulfoxide (DMSO) at room temperature for 1 h, after which it was rinsed with DMSO, ethanol, and DI water in sequence. Subsequently, 10 μM PNA was dropped onto the chip surface and incubated at room temperature for 2 h. To remove unreacted probe, 1 × PBS solutions containing 0.2% SDS, 1 × PBS, and DI water were successively used. PASE is able to cross-link PNA only to the graphene, because a $\pi-\pi$ stacking interaction occurs between PASE and the graphene surface, whereas there is no $\pi-\pi$ stacking interaction between the chip surface (SiO_2 interface) and PASE. Finally, the chip was treated with 100 mM ethanolamine (EA) solution (pH 9.0) for 1 h to avoid possible nonspecific adsorption on the graphene surface and then rinsed with DI water.

PNA–DNA Hybridization. The complementary probe DNA was added on top of the biosensor array surface after PNA functionalization, and incubation was allowed for 1 h to ensure a sufficient PNA–DNA hybridization reaction. Subsequently, the chip was rinsed with 1 × PBS solutions containing 0.2% SDS, 1 × PBS, and DI water successively and then dried with N_2. The same operation process was applied for the one-base-mismatched and noncomplementary DNA sequences for hybridization with the PNA probe.

Electrical Measurements. All electrical measurements were obtained on a Keithley 4200 semiconductor characterization system combined with a probe station (EverBeing BD-6). For transfer curve measurements of the FET biosensor, solution-gate experiments were carried out using silver wire reference electrodes as a gate electrode immersed in buffer solution and a constant bias V_{DS} = 0.1 V (drain–source voltage) was applied. Output curves were measured at assigned V_G (gate voltage) value.

Characterizations. The transferred SLG was characterized using both optical microscopy (ZEISS Axio scope A1) and Raman microscopy (LabRAM HR 800). Raman spectrum of the samples was taken with the Raman microscopy system equipped with 633 nm laser. JSM-6510 LV scanning electron microscopy (SEM) was used for SEM characterization of the device. The X-ray photoelectron spectroscopy was performed on an ESCALAB 250 Xi XPS system (Thermo Fisher Scientific) equipped with a monochromatic Al Kα source radiation.

RESULTS AND DISCUSSION

Panels a and b of Figure 1 show optical images of FET devices fabricated on a 4-in. wafer containing 110 devices and an individual FET device, respectively. Figure 1c shows SEM images of the six sensor arrays of an individual FET device. The size of the whole device was 6 × 4.5 mm, and the width of the sensing channel was 4 μm between the two electrodes.

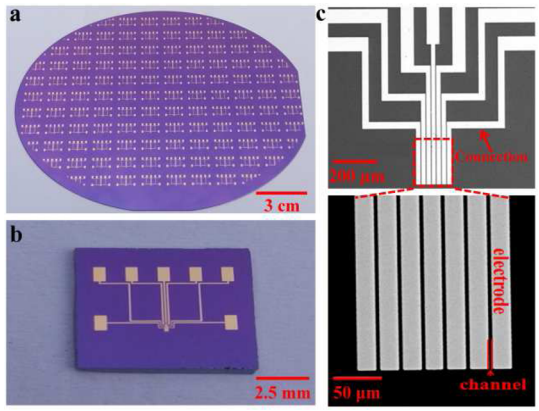

Figure 1. (a) Optical image of FET devices fabricated on a 4-in. wafer. (b) Optical image of an individual FET device. (c) SEM images of the sensor arrays of an individual FET device.

Figure 2a shows optical images of the transferred graphene between two electrodes, indicating that monolayer graphene covered the whole channel.[35] The graphene after directional transfer was further characterized by Raman microscopy. The Raman spectrum of the as-transferred graphene sample indicated high-quality monolayer graphene, as it was found to have a high I_{2D}/I_G ratio of 2.43 (Figure 2b).[18,36] The results demonstrated that the graphene transferred onto the fabricated FET sensor chip was a monolayer.

It is notable that there was no effect on the measurements even though the contact lines of the chips were not passivated. As can be seen from Figure S1, the drain current was 3 orders of magnitude higher than the gate leakage. Therefore, the effect was negligible even though the contact lines were not passivated. Electrical measurements were obtained before and after annealing. As can be seen in Figure 3a, the right shift of the charge-neutrality point (V_{CNP}) indicated that the carrier density of graphene increased (p-doped) after thermal annealing.[23] From the plot of the drain–source current (I_{DS}) versus the gate voltage (V_G) in Figure 3b, the FET with the as-transferred graphene had a Dirac-point voltage of 0.4 V and a very small hysteresis of 2 mV, pointing to the fact that the fabrication process was clean and harmless to graphene. The p-type doping is attributed to graphene exposed to the ambient environment and subsequently thermal annealing.[23,37,38] The output characteristics in Figure S2 show that the drain current decreased when the gate voltage was increased from −0.3 to 0.3 V, again indicating that the device was p-type doped. The results are consistent with the previous results, and the drain response is sensitive to the change in gate voltage.

As is known, it is important to wash PMMA away and make the transferred graphene clean. Therefore, PMMA was washed away with hot acetone and annealing in this work. Three pieces of evidence support the clean graphene surface. First, Raman spectroscopy is a potential method for tracing residual PMMA on the graphene surface. Figure S3 shows a typical Raman

DOI: 10.1021/acsami.5b03941
ACS Appl. Mater. Interfaces 2015, 7, 16953–16959

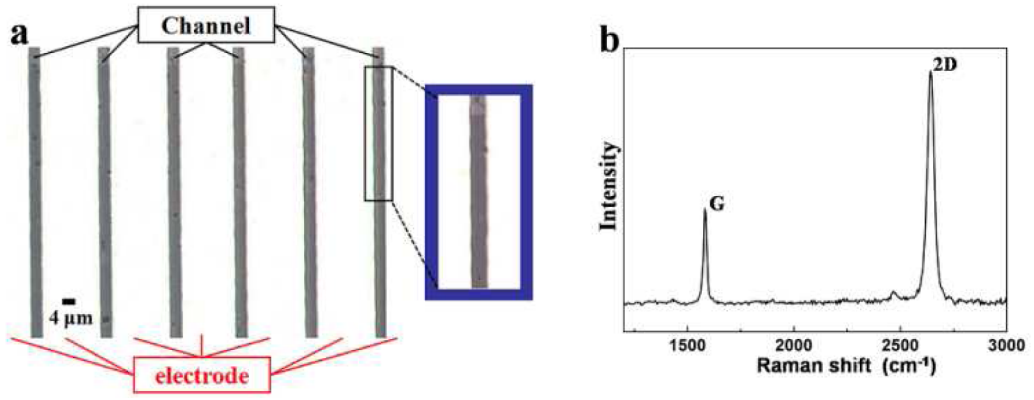

Figure 2. (a) Metallurgical microscopy images showing six individual sensor channels coated with the CVD SLG spanning across Au electrodes. (b) Raman spectrum of the CVD SLG prepared by the directional transfer technique, indicating that the transferred graphene was a single layer.

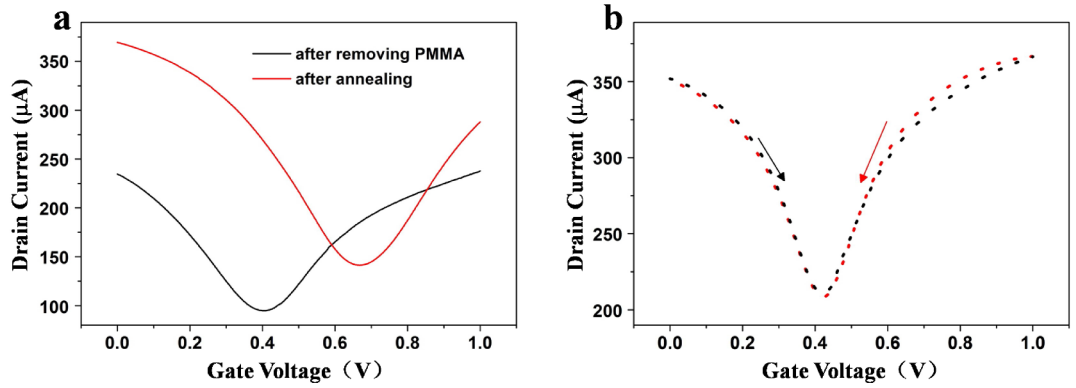

Figure 3. (a) Transfer characteristics of a solution-gate SLG FET before and after thermal annealing. (b) I_{DS}–V_G transfer curves of a CVD-grown SLG FET device with a constant V_{DS} of 0.1 V in solution. The arrows refer to the direction of the gate voltage sweep. The black and red lines represent the transfer characteristic curves when the gate bias was swept forward and backward, respectively, between 0 and 1 V.

spectrum of PMMA residue on graphene. The two peaks at 1450 and 1530 cm^{-1} can be attributed to the effect of PMMA residue on the graphene surface (Figure S3)[34]. On the contrary, the two additional peaks disappeared after the PMMA was washed away, as shown in Figure 2b, indicating that the graphene surface is clean. Second, the transfer characteristics curve (Figure 3b) shows a very small hysteresis of 2 mV, further confirming that the graphene surface was clean. Finally, X-ray photoelectron spectroscopy (XPS) was further conducted to trace the PMMA residue on graphene. Figure S4 shows the evolution of the C 1s core-level spectra of the PMMA residue on graphene and of clean graphene. The black line represents the raw spectrum. To fit the C 1s XPS spectra, the sp^2 component of C—C bonding was obtained by using the asymmetric Gaussian–Lorentzian formula. The main peak (red line) was attributed to the graphene sp^2 components of the post-transfer C 1s spectrum. Compared to the XPS spectrum of clean graphene (Figure S4b), both the C—O peak (magenta line) and the C═O peak (purple line) appeared (Figure S4a), corresponding to the binding energies of species of PMMA residue on graphene in addition to the main peak. Therefore, it is clear that PMMA was completely removed from the graphene surface by hot acetone and annealing. Based on the described evidence, the G-FET biosensors fabricated by the directional transfer technique were clean.

The principle of the SLG FET biosensor for DNA detection is same as that reported previously.[10] Briefly, the G-FET arrays are functionalized with PNA by the linker molecule PASE through π–π stacking interactions between the pyrene groups and the graphene surface. The specific target DNA is then hybridized with the immobilized PNA. For electrical measurements, 0.01 × PBS buffer solution is dropped onto the biosensor, and a silver wire as a liquid gate is immersed in the buffer solution to offer a gate voltage. A negative shift in the V_{CNP} value of graphene upon PNA/DNA hybridization was observed, and the imposition of n-doping on the graphene by the electron-rich nucleobases in the DNA strand is considered as the detection mechanism.[2,39,40] The specific detection of target DNA using a CVD-grown SLG FET biosensor was investigated by applying various target DNA concentrations to the PNA-functionalized FET biosensor. To exclude the possibility of nonspecific adsorption and false signals, a series of control experiments were carried out. First, it was necessary to measure the influence of 1 × PBS on the biosensing ability because the target DNA was dissolved in 1 × PBS. The transfer characteristics curves were found to exhibit negligible change before and after 1 × PBS buffer solution was incubated with the PNA-functionalized FET biosensor (Figure 4a). Second, it is known from previous reports that graphene-oxide-category-based biosensors usually present obvious nonspecific adsorption.[41] In this research, as observed in Figure 4b, the transfer curves exhibited minimal change after the FET biosensor without PNA modification was incubated with 10 fM cDNA, 1 pM cDNA, and 100 pM cDNA. Compared to RGO, CVD-grown SLG graphene does not contain functional groups and is inert to biomolecules. Figure 4c shows the transfer character-

DOI: 10.1021/acsami.5b03941
ACS Appl. Mater. Interfaces 2015, 7, 16953–16959

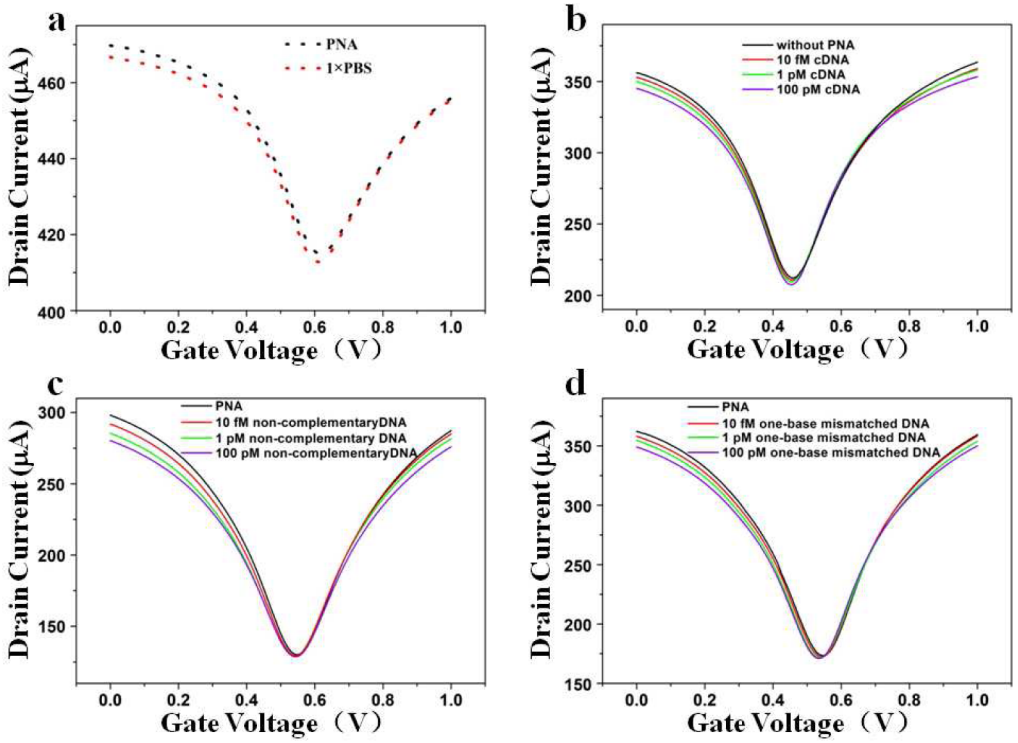

Figure 4. (a) Transfer characteristics of a PNA-functionalized CVD SLG FET biosensor incubated with 1 × PBS buffer solution, as a blank control. (b) Transfer characteristics of a CVD SLG FET biosensor without PNA modification hybridized with 1 × PBS and 10 fM, 1 pM, and 100 pM complementary target DNA (cDNA). (c) V_{CNP} shifts of PNA-immobilized CVD SLG FET biosensors hybridized with different concentrations of noncomplementary DNA. (d) V_{CNP} shifts of PNA-immobilized CVD SLG FET biosensors hybridized with different concentrations of one-base mismatch DNA target.

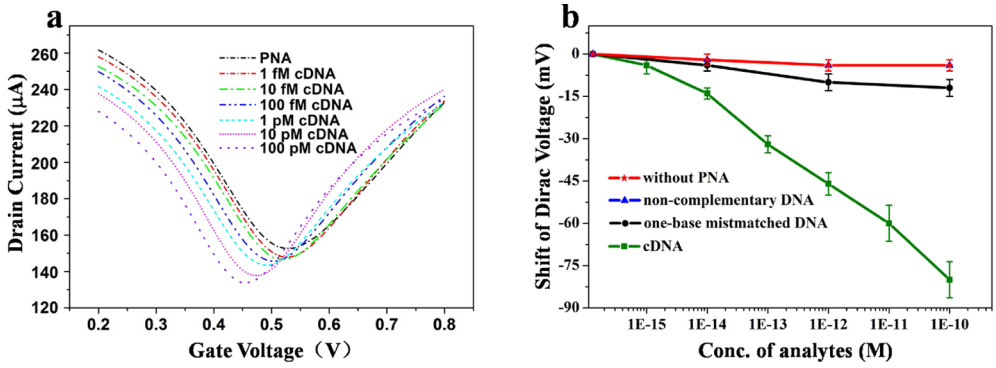

Figure 5. (a) V_{CNP} shifts of PNA-immobilized CVD SLG FET biosensors hybridized with complementary DNA target with concentrations ranging from 1 fM to 100 pM. (b) Summary of V_{CNP} shifts of the CVD SLG FET biosensor: the FET biosensor without PNA modification upon hybridization with various concentrations of complementary DNA target and the PNA-immobilized FET biosensor upon hybridization with various concentrations of complementary, noncomplementary, and one-base-mismatched DNA targets.

istics curves of the PNA-immobilized CVD-grown SLG FET biosensors incubated with 10 fM non-DNA, 1 pM non-DNA, and 100 pM non-DNA. As illustrated, the shift in V_{CNP} was again negligible, indicating that there was no hybridization between PNA and non-DNA. Figure 4d shows that the shift of V_{CNP} for PNA-immobilized SLG FET biosensors incubated with 10 fM, 1 pM, and 100 pM one-base-mismatched DNA, respectively. At very low concentrations of one-base-mismatched DNA, a shift in V_{CNP} was hardly observed. However, the shift inV_{CNP} at 100 pM was found to be obvious and much larger than that for non-DNA. For one-base mismatch, a duplex can still be formed between the one-base-mismatched DNA and the probe PNA, although the duplex is unstable and most of the duplexes formed can be unzipped during the washing steps. Therefore, compared to complementary and non-complementary DNA, the signal is either lower or higher, respectively.

Next, to investigate the sensitivity of the CVD-grown SLG FET biosensor, various concentrations of target DNA were sequentially incubated with the PNA-immobilized SLG FET biosensors. As shown in Figure 5a, the V_{CNP} value of the devices shifted toward the negative gate voltage as the concentration of cDNA was increased from 1 fM to 100 pM. The larger the shift, the higher the concentration. This result is in good agreement with those reported in the literature.[2,23,39] Figure 5b summarizes the V_{CNP} shifts versus cDNA, non-DNA, one-base-mismatched DNA, and blank control PBS buffer. These data confirm that the developed FET biosensors can well

DOI: 10.1021/acsami.5b03941
ACS Appl. Mater. Interfaces 2015, 7, 16953−16959

distinguish complementary DNA from one-base-mismatched DNA and noncomplementary DNA, and they can certainly be used for the detection of single nucleotide polymorphism (SNP). Therefore, the CVD-grown SLG FET biosensors present a high specificity for DNA detection. The detection limit of the FET biosensors was as low as 10 fM for DNA detection based on the signals that surpass the background by a factor of 3. The detection limit is 2 orders of magnitude lower than that reported by Chen et al.[23] and 1 order of magnitude lower than that reported by Cai et al.[10] The high sensitivity can be attributed to usage of monolayer graphene as the channel material, as well as PNA as the probe. As mentioned earlier, because PNA has a nonionic backbone,[42,43] electrostatic repulsion between PNA−DNA hybridized strands is reduced, thereby lowering the background signal and improving detection sensitivity.[44] On the other hand, the quality of graphene basically affects the sensitivity of the FET biosensor. The graphene transferred to the FET device was a monolayer, with a high surface-to-volume ratio and thereby a high detection sensitivity. The carrier mobility is an important parameter for determining graphene quality, although there is no direct relation between mobility and the shift of Dirac point. In this work, we obtained the mobility of graphene by the directional transfer technique based on the following equation without considering the contact resistance: $\mu = (1/C_{ox})(L/W)(g_m/V_{DS})$, where $g_m = \Delta I_{DS}/\Delta V_G = (W/L)\mu C_{ox}V_{DS}$ is the peak transconductance, L is the length of the device between source and drain, W is the width of the device, and C_{ox} is the capacitance of the insulating layer between the gate insulator and the conducting graphene channel. The mobility was found to be 605 $cm^2\ V^{-1}\ s^{-1}$, which is much higher than that of the RGO-based FET biosensors[45,46] but lower than that of a CVD-grown graphene nanoribbon FET biosensor.[28] Dong et al.[45] reported a label-free DNA FET biosensor based on RGO and gold-nanoparticle-modified RGO (Au-RGO) in which the mobilities of RGO and Au-RGO were about 0.015 and 9 $cm^2\ V^{-1}\ s^{-1}$, respectively. However, the sensitivity in that work was not reported. Hasegawa et al.[46] fabricated a RGO-based FET biosensor for immunoglobulin E (IgE) detection, in which the mobility of RGO was around 6 $cm^2\ V^{-1}\ s^{-1}$ and the IgE detection limit was 8.1 ng/mL. Lerner et al.[28] proposed a transfer method of patterning a CVD-grown graphene nanoribbon for scalable production of nanosensors to detect naltrexone with a high sensitivity (10 pg/mL), in which the mobility of the CVD-grown graphene nanoribbon was, on average, 1500 $cm^2\ V^{-1}\ s^{-1}$. This comparison clearly shows that the transferred SLG had a high quality and that the developed SLG FET biosensor is capable of achieving a high sensitivity.

The reproducibility of DNA sensing was investigated by calculating the relative standard deviation (RSD) for independent SLG FET biosensors. The RSD value was found to be 8.5%, demonstrating a satisfactory chip-to-chip variation.

Finally, the reusability of the SLG FET biosensor was also investigated (Figure S5). The experimental process was performed as mentioned in the previous report.[10] The target was chosen to be 1 pM complementary DNA. After three cycles of denaturation and rehybridization, the hybridization signal percentages of the second and third hybridizations were found to be 86% and 76%, respectively, of the first-cycle hybridization signal, indicating that the SLG FET biosensor had good reusability and could be reused multiple times.

CONCLUSIONS

In conclusion, we have developed a novel FET nanobiosensor based on CVD-grown monolayer graphene transferred to the device by the directional technique and high-affinity PNA−DNA hybridization for ultrasensitive, label-free, and highly specific detection of DNA. Rapid production of the CVD-grown monolayer graphene FET biosensor was achieved by the simple directional transfer technique. Compared to previously published works, the fabricated CVD-grown SLG FET biosensor showed a great sequence-specific affinity to the target DNA and achieved an excellent DNA detection sensitivity as high as 10 fM. Moreover, this FET nanobiosensor could also discriminate complementary DNA from one-base-mismatched DNA and noncomplementary DNA with high specificity. In addition, the SLG FET biosensor showed satisfactory reproducibility and stability. This report could further promote the development of graphene transfer techniques and pave a progressive avenue to design and fabricate novel electronic nanobiosensors for ultrasensitive and highly specific detection of DNA in disease diagnostics.

ASSOCIATED CONTENT

Supporting Information

The Supporting Information is available free of charge on the ACS Publications website at DOI: 10.1021/acsami.5b03941.

Detailed descriptions of the conventional transfer technique process for fabrication of a G-FET biosensor, Raman and XPS characterization of graphene surface, electrical properties of G-FET, and reusability of the SLG G-FET biosensors (PDF)

AUTHOR INFORMATION

Corresponding Authors

*Tel.: +86-27-68890259. Fax: +86-27-68890259. E-mail: zhanggj@hbtcm.edu.cn (G.-J.Z.).
*E-mail: zyzhang@pku.edu.cn (Z.Z.).

Notes

The authors declare no competing financial interest.

ACKNOWLEDGMENTS

This work was supported by the National Natural Science Foundation of China (Nos. 21275040, 21475034, and 21405037) and the Natural Science Foundation of Hubei Province (No. 2013CFA061).

REFERENCES

(1) Novoselov, K. S.; Geim, A. K.; Morozov, S.; Jiang, D.; Zhang, Y.; Dubonos, S.; Grigorieva, I.; Firsov, A. Electric Field Effect in Atomically Thin Carbon Films. *Science* **2004**, *306*, 666−669.
(2) Dong, X.; Shi, Y.; Huang, W.; Chen, P.; Li, L. J. Electrical Detection of DNA Hybridization with Single-Base Specificity Using Transistors Based on CVD-Grown Graphene Sheets. *Adv. Mater.* **2010**, *22*, 1649−1653.
(3) Lin, Y. M.; Avouris, P. Strong Suppression of Electrical Noise in Bilayer Graphene Nanodevices. *Nano Lett.* **2008**, *8*, 2119−2125.
(4) Drummond, T. G.; Hill, M. G.; Barton, J. K. Electrochemical DNA Sensors. *Nat. Biotechnol.* **2003**, *21*, 1192−1199.
(5) Hay Burgess, D. C.; Wasserman, J.; Dahl, C. A. Global Health Diagnostics. *Nature* **2006**, *444*, 1−2.
(6) Du, Y.; Guo, S.; Dong, S.; Wang, E. An Integrated Sensing System for Detection of DNA Using New Parallel-Motif DNA Triplex System and Graphene-Mesoporous Silica−Gold Nanoparticle Hybrids. *Biomaterials* **2011**, *32*, 8584−8592.

DOI: 10.1021/acsami.5b03941
ACS Appl. Mater. Interfaces 2015, 7, 16953−16959

(7) Guo, S.; Du, D.; Tang, L.; Ning, Y.; Yao, Q.; Zhang, G. J. PNA-Assembled Graphene Oxide for Sensitive and Selective Detection of DNA. *Analyst* **2013**, *138*, 3216−3220.
(8) Du, D.; Guo, S.; Tang, L.; Ning, Y.; Yao, Q.; Zhang, G. J. Graphene-Modified Electrode for DNA Detection via PNA−DNA Hybridization. *Sens. Actuators, B* **2013**, *186*, 563−570.
(9) Star, A.; Tu, E.; Niemann, J.; Gabriel, J. C. P.; Joiner, C. S.; Valcke, C. Label-Free Detection of DNA Hybridization Using Carbon Nanotube Network Field-Effect Transistors. *Proc. Natl. Acad. Sci. U. S. A.* **2006**, *103*, 921−926.
(10) Cai, B.; Wang, S.; Huang, L.; Ning, Y.; Zhang, Z.; Zhang, G. J. Ultrasensitive Label-Free Detection of PNA−DNA Hybridization by Reduced Graphene Oxide Field-Effect Transistor Biosensor. *ACS Nano* **2014**, *8*, 2632−2638.
(11) Geim, A. K. Graphene: Status and Prospects. *Science* **2009**, *324*, 1530−1534.
(12) Ohno, Y.; Maehashi, K.; Matsumoto, K. Chemical and Biological Sensing Applications Based on Graphene Field-Effect Transistors. *Biosens. Bioelectron.* **2010**, *26*, 1727−1730.
(13) Hummers, W. S.; Offeman, R. E. Preparation of Graphitic Oxide. *J. Am. Chem. Soc.* **1958**, *80*, 1339−1339.
(14) Si, Y.; Samulski, E. T. Synthesis of Water Soluble Graphene. *Nano Lett.* **2008**, *8*, 1679−1682.
(15) Mohanty, N.; Berry, V. Graphene-Based Single-Bacterium Resolution Biodevice and DNA Transistor: Interfacing Graphene Derivatives with Nanoscale and Microscale Biocomponents. *Nano Lett.* **2008**, *8*, 4469−4476.
(16) Li, X.; Cai, W.; An, J.; Kim, S.; Nah, J.; Yang, D.; Piner, R.; Velamakanni, A.; Jung, I.; Tutuc, E.; Banerjee, S. K.; Colombo, L.; Ruoff, R. S. Large-Area Synthesis of High-Quality and Uniform Graphene Films on Copper Foils. *Science* **2009**, *324*, 1312−1314.
(17) Sutter, P. W.; Flege, J. I.; Sutter, E. A. Epitaxial Graphene on Ruthenium. *Nat. Mater.* **2008**, *7*, 406−411.
(18) Reina, A.; Jia, X.; Ho, J.; Nezich, D.; Son, H.; Bulovic, V.; Dresselhaus, M. S.; Kong, J. Large Area, Few-Layer Graphene Films on Arbitrary Substrates by Chemical Vapor Deposition. *Nano Lett.* **2009**, *9*, 30−35.
(19) Stine, R.; Robinson, J. T.; Sheehan, P. E.; Tamanaha, C. R. Real-Time DNA Detection Using Reduced Graphene Oxide Field Effect Transistors. *Adv. Mater.* **2010**, *22*, 5297−5300.
(20) He, Q.; Wu, S.; Gao, S.; Cao, X.; Yin, Z.; Li, H.; Chen, P.; Zhang, H. Transparent, Flexible, All-Reduced Graphene Oxide Thin Film Transistors. *ACS Nano* **2011**, *5*, 5038−5044.
(21) Guo, S. R.; Lin, J.; Penchev, M.; Yengel, E.; Ghazinejad, M.; Ozkan, C. S.; Ozkan, M. Label Free DNA Detection Using Large Area Graphene Based Field Effect Transistor Biosensors. *J. Nanosci. Nanotechnol.* **2011**, *11*, 5258−5263.
(22) Dong, X.; Fu, D.; Xu, Y.; Wei, J.; Shi, Y.; Chen, P.; Li, L. J. Label-Free Electronic Detection of DNA Using Simple Double-Walled Carbon Nanotube Resistors. *J. Phys. Chem. C* **2008**, *112*, 9891−9895.
(23) Chen, T. Y.; Loan, P. T. K.; Hsu, C. L.; Lee, Y. H.; Tse-Wei Wang, J.; Wei, K. H.; Lin, C. T.; Li, L. J. Label-Free Detection of DNA Hybridization Using Transistors Based on CVD Grown Graphene. *Biosens. Bioelectron.* **2013**, *41*, 103−109.
(24) Xu, G.; Abbott, J.; Qin, L.; Yeung, K. Y.; Song, Y.; Yoon, H.; Kong, J.; Ham, D. Electrophoretic and Field-Effect Graphene for All-Electrical DNA Array Technology. *Nat. Commun.* **2014**, *5*, 4866.
(25) Colombo, L.; Wallace, R. M.; Ruoff, R. S. Graphene Growth and Device Integration. *Proc. IEEE* **2013**, *101*, 1536−1556.
(26) Hess, L. H.; Seifert, M.; Garrido, J. A. Graphene Transistors for Bioelectronics. *Proc. IEEE* **2013**, *101*, 1780−1792.
(27) Hess, L. H.; Jansen, M.; Maybeck, V.; Hauf, M. V.; Seifert, M.; Stutzmann, M.; Sharp, I. D.; Offenhäusser, A.; Garrido, J. A. Graphene Transistor Arrays for Recording Action Potentials from Electrogenic Cells. *Adv. Mater.* **2011**, *23*, 5045−5049.
(28) Lerner, M. B.; Matsunaga, F.; Han, G. H.; Hong, S. J.; Xi, J.; Crook, A.; Perez-Aguilar, J. M.; Park, Y. W.; Saven, J. G.; Liu, R.; Johnson, A. T. C. Scalable Production of Highly-Sensitive Nanosensors Based on Graphene Functionalized with a Designed G Protein-Coupled Receptor. *Nano Lett.* **2014**, *14*, 2709−2714.
(29) Shi, R.; Xu, H.; Chen, B.; Zhang, Z.; Peng, L. M. Scalable Fabrication of Graphene Devices through Photolithography. *Appl. Phys. Lett.* **2013**, *102*, 113102.
(30) Lin, W. H.; Chen, T. H.; Chang, J. K.; Taur, J. I.; Lo, Y. Y.; Lee, W. L.; Chang, C. S.; Su, W. B.; Wu, C. I. A Direct and Polymer-Free Method for Transferring Graphene Grown by Chemical Vapor Deposition to Any Substrate. *ACS Nano* **2014**, *8*, 1784−1791.
(31) Chan, J.; Venugopal, A.; Pirkle, A.; McDonnell, S.; Hinojos, D.; Magnuson, C. W.; Ruoff, R. S.; Colombo, L.; Wallace, R. M.; Vogel, E. M. Reducing Extrinsic Performance-Limiting Factors in Graphene Grown by Chemical Vapor Deposition. *ACS Nano* **2012**, *6*, 3224−3229.
(32) Huang, L.; Xu, H.; Zhang, Z.; Chen, C.; Jiang, J.; Ma, X.; Chen, B.; Li, Z.; Zhong, H.; Peng, L. M. Graphene/Si CMOS Hybrid Hall Integrated Circuits. *Sci. Rep.* **2014**, *4*, 5548.
(33) Suk, J. W.; Kitt, A.; Magnuson, C. W.; Hao, Y.; Ahmed, S.; An, J.; Swan, A. K.; Goldberg, B. B.; Ruoff, R. S. Transfer of CVD-Grown Monolayer Graphene onto Arbitrary Substrates. *ACS Nano* **2011**, *5*, 6916−6924.
(34) Lin, Y. C.; Jin, C.; Lee, J. C.; Jen, S. F.; Suenaga, K.; Chiu, P. W. Clean Transfer of Graphene for Isolation and Suspension. *ACS Nano* **2011**, *5*, 2362−2368.
(35) Blake, P.; Hill, E.; Castro Neto, A. H.; Novoselov, K.; Jiang, D.; Yang, R.; Booth, T.; Geim, A. Making Graphene Visible. *Appl. Phys. Lett.* **2007**, *91*, 063124.
(36) Pimenta, M.; Dresselhaus, G.; Dresselhaus, M. S.; Cançado, L.; Jorio, A.; Saito, R. Studying Disorder in Graphite-Based Systems by Raman Spectroscopy. *Phys. Chem. Chem. Phys.* **2007**, *9*, 1276−1290.
(37) Wang, X.; Li, X.; Zhang, L.; Yoon, Y.; Weber, P. K.; Wang, H.; Guo, J.; Dai, H. N-Doping of Graphene through Electrothermal Reactions with Ammonia. *Science* **2009**, *324*, 768−771.
(38) Jung, I.; Dikin, D. A.; Piner, R. D.; Ruoff, R. S. Tunable Electrical Conductivity of Individual Graphene Oxide Sheets Reduced at "Low" Temperatures. *Nano Lett.* **2008**, *8*, 4283−4287.
(39) Lin, C. T.; Loan, P. T. K.; Chen, T. Y.; Liu, K. K.; Chen, C. H.; Wei, K. H.; Li, L. J. Label-Free Electrical Detection of DNA Hybridization on Graphene Using Hall Effect Measurements: Revisiting The Sensing Mechanism. *Adv. Funct. Mater.* **2013**, *23*, 2301−2307.
(40) Manohar, S.; Mantz, A. R.; Bancroft, K. E.; Hui, C. Y.; Jagota, A.; Vezenov, D. V. Peeling Single-Stranded DNA from Graphite Surface to Determine Oligonucleotide Binding Energy by Force Spectroscopy. *Nano Lett.* **2008**, *8*, 4365−4372.
(41) Zhang, X.; Zhang, Y.; Liao, Q.; Song, Y.; Ma, S. Reduced Graphene Oxide-Functionalized High Electron Mobility Transistors for Novel Recognition Pattern Label-Free DNA Sensors. *Small* **2013**, *9*, 4045−4050.
(42) Nielsen, P. E.; Egholm, M.; Berg, R. H.; Buchardt, O. Sequence-Selective Recognition of DNA by Strand Displacement with A Thymine-Substituted Polyamide. *Science* **1991**, *254*, 1497−1500.
(43) Nielsen, P. E.; Egholm, M.; Buchardt, O. Peptide Nucleic Acid (PNA). A DNA Mimic with A Peptide Backbone. *Bioconjugate Chem.* **1994**, *5*, 3−7.
(44) Zhang, G. J.; Chua, J. H.; Chee, R. E.; Agarwal, A.; Wong, S. M.; Buddharaju, K. D.; Balasubramanian, N. Highly Sensitive Measurements of PNA−DNA Hybridization Using Oxide-Etched Silicon Nanowire Biosensors. *Biosens. Bioelectron.* **2008**, *23*, 1701−1707.
(45) Dong, X.; Huang, W.; Chen, P. In Situ Synthesis of Reduced Graphene Oxide and Gold Nanocomposites for Nanoelectronics and Biosensing. *Nanoscale Res. Lett.* **2011**, *6*, 60.
(46) Hasegawa, M.; Hirayama, Y.; Ohno, Y.; Maehashi, K.; Matsumoto, K. Characterization of Reduced Graphene Oxide Field-Effect Transistor and Its Application to Biosensor. *Jpn. J. Appl. Phys.* **2014**, *53*, 05FD05.

DOI: 10.1021/acsami.5b03941
ACS Appl. Mater. Interfaces 2015, 7, 16953−16959